DOI: 10.1002/pul2.12368

RESEARCH ARTICLE

Pulmonary Circulation PVRI WILEY

Exploratory analysis of the accuracy of echocardiographic parameters for the assessment of right ventricular function and right ventricular–pulmonary artery coupling

Hideki Shima[1] | Ichizo Tsujino[1,2] | Junichi Nakamura[1] |
Toshitaka Nakaya[1] | Ayako Sugimoto[1] | Takahiro Sato[1,2] | Taku Watanabe[1] |
Hiroshi Ohira[1] | Masaru Suzuki[1] | Satonori Tsuneta[3] | Yasuyuki Chiba[4] |
Michito Murayama[5,6] | Isao Yokota[7] | Satoshi Konno[1,2]

[1]Department of Respiratory Medicine, Faculty of Medicine, Hokkaido University, Sapporo, Japan

[2]Division of Respiratory and Cardiovascular Innovative Research, Faculty of Medicine, Hokkaido University, Sapporo, Japan

[3]Department of Diagnostic and Interventional Radiology, Hokkaido University Hospital, Sapporo, Japan

[4]Department of Cardiovascular Medicine, Hokkaido University Graduate School of Medicine, Sapporo, Japan

[5]Department of Medical Laboratory Science, Faculty of Health Sciences, Hokkaido University, Sapporo, Japan

[6]Diagnostic Center for Sonography, Hokkaido University Hospital, Sapporo, Japan

[7]Department of Biostatistics, Hokkaido University Graduate School of Medicine, Sapporo, Japan

Correspondence
Ichizo Tsujino, Division of Respiratory and Cardiovascular Innovative Research,

Abstract

Echocardiography is a widely used modality for the assessment of right ventricular (RV) function; however, few studies have comprehensively compared the accuracy of echocardiographic parameters using invasively obtained reference values. Therefore, this exploratory study aimed to compare the accuracy of echocardiographic parameters of RV function and RV–pulmonary artery (PA) coupling. We calculated four indices of RV function (end-systolic elastance [Ees] for systolic function [contractility], τ for relaxation, and β and end-diastolic elastance [Eed] for stiffness), and an index of RV–PA coupling (Ees/arterial elastance [Ea]), using pressure catheterization, cardiac magnetic resonance imaging, and a single-beat method. We then compared the correlations of RV indices with echocardiographic parameters. In 63 participants (54 with pulmonary hypertension (PH) and nine without PH), Ees and τ correlated with several echocardiographic parameters, such as RV diameter and area, but the correlations were moderate (|correlation coefficients (ρ)| < 0.5 for all parameters). The correlations of β and Eed with echocardiographic parameters were weak, with $|\rho| < 0.4$. In contrast, Ees/Ea closely correlated with RV free wall longitudinal strain (RVFW-LS)/estimated systolic PA pressure (eSPAP) ($\rho = -0.72$). Ees/Ea also correlated with tricuspid

Faculty of Medicine, Hokkaido
University, N15, W7, Kita-ku, Sapporo,
Hokkaido 060-8638, Japan.
Email: itsujino@med.hokudai.ac.jp

annular plane systolic excursion/eSPAP, RV diameter, and RV end-systolic area, with $|\rho| > 0.65$. In addition, RVFW-LS/eSPAP yielded high sensitivity (0.84) and specificity (0.75) for detecting reduced Ees/Ea. The present study indicated a limited accuracy of echocardiographic parameters in assessing RV systolic and diastolic function. In contrast to RV function, they showed high accuracy for assessing RV–PA coupling, with RVFW-LS/eSPAP exhibiting the highest accuracy.

KEYWORDS
magnetic resonance imaging, pressure catheter, pulmonary artery, pulmonary hypertension, single beat method

INTRODUCTION

Pulmonary hypertension (PH) is hemodynamically defined by an elevated mean pulmonary arterial (PA) pressure of ≥25 mmHg[1,2] or >20 mmHg in the updated guidelines.[3] In PH, a sustained elevation of PA pressure or the afterload of the right ventricle impairs right ventricular (RV) function and its adaptation to the pulmonary vascular system, that is, RV–PA coupling.[4] Notably, the presence and degree of impaired RV function and of RV–PA coupling are considered to affect the outcomes of patients with PH.[5–7] Therefore, accurate evaluation of RV function and RV–PA coupling is essential for the precise assessment and optimal management of patients.

The gold standard for evaluating RV function and RV–PA coupling is the multibeat method performed using conductance and pressure catheters.[8,9] This method enables simultaneous monitoring of RV volume and pressure, and the calculated values and their clinical relevance have been reported.[10,11] However, owing to the cost, invasiveness, and need for special equipment, such analyses can only be performed at a few facilities, reducing its application in the practice.

A simpler way of evaluating RV function is using the single-beat method,[12,13] with the application of a pressure catheter and cardiac magnetic resonance (CMR) imaging.[14] RV indices obtained using this method are associated with the prognosis of patients with PH.[15,16] In particular, end systolic elastance (Ees) divided by arterial elastance (Ea) (Ees/Ea), an index of RV–PA coupling, is most closely associated with the outcome of patients with PH.[15,16] However, even with this simplified method, such indices are still challenging to use in the clinical practice, because of the need for dedicated software and mathematical processing.

As echocardiography is noninvasive, it can be performed repeatedly. Various echocardiographic indices are considered to reflect RV function and RV–PA coupling and are widely used in clinical practice.[17,18] However, the correlations of such indices with invasively measured reference values have been reported in a small number of studies.[6,19–21] In addition, these studies focused on only one or a few echocardiographic parameters, and their accuracy was not comprehensively compared with that of other parameters. As a result, it remains unclear which parameter most accurately reflects RV systolic/diastolic function and RV–PA coupling.

The primary purpose of this study was to comprehensively compare the accuracy of echocardiographic parameters of RV function and RV–PA coupling, using pressure catheter, CMR, and single-beat method-derived data as reference values. In addition, for the echocardiographic parameters that provided good accuracy, we aimed to exploratory determine their sensitivity and specificity for detecting impaired RV function or RV–PA coupling.

METHODS

Study population

Of the patients admitted to our department for PH diagnosis or follow-up from May 2020 to April 2022, those who underwent right heart catheterization (RHC) with a pressure catheter, echocardiography, and CMR imaging within 14 days before and after RHC were retrospectively evaluated. Clinically unstable patients with modifications to their PH medication during the abovementioned ±14 days from RHC and those with a left ventricular (LV) ejection fraction (EF) < 50% upon echocardiography were excluded. The diagnostic criteria and treatment strategies for PH were defined according to the 2015 European and 2017 Japanese PH treatment

guidelines.[1,22] Hence, a mean PA pressure (MPAP) ≥ 25 mmHg was used to define PH.

This study was approved by the Ethics Committee of Hokkaido University Hospital (Approval number: 016-0461) and conducted in accordance with the 1964 Declaration of Helsinki and its subsequent amendments. As this was a retrospective study, the need for informed consent was waived by the Ethics Committee. However, patients could opt out of the study and they were informed of this right on our institutional website.

RHC

RHC was performed according to the guidelines at the time of practice.[23] Briefly, a Swan–Ganz catheter was used to measure PA pressure, PA wedge pressure, cardiac output, RV pressure (RVP), and right atrial (RA) pressure.

Immediately after Swan–Ganz catheterization, a pressure catheter (Mikro-Cath pressure catheter; Millar Co. Ltd) was inserted and advanced to the PA. Subsequently, as reported in our previous study,[24] PAP and RVP were recorded using an AV converter (Power-Lab; ADInstruments) and a dedicated software (Lab-Chart Pro; ADInstruments).

CMR imaging

CMR imaging studies were performed on a 1.5-T magnetic resonance imaging (MRI) scanner (Achieva or Achieva dStream; Philips Healthcare) or a 3.0-T MRI scanner (Achieva TX; Philips Medical Systems) with electrocardiogram gating. Image acquisition and analysis were performed using a previously described protocol.[24] Briefly, cine MRI was performed in the axial plane covering the whole heart, using a steady-state free precession pulse sequence. The details of the parameters are provided in Supporting Information S12: Table 1. Images were analyzed using a dedicated software (Extended MR WorkSpace or IntelliSpace Portal; Philips Healthcare). The endocardial contours were manually traced, and the RV and LV end-diastolic volumes (EDVs) and end-systolic volumes (ESVs) were computed. The RV and LV stroke volume (SV) and EF were calculated as $SV = EDV - ESV$ and $EF = SV/EDV \times 100\%$, respectively.

Echocardiography

Transthoracic echocardiography was performed using the Artida/Aplio i900 (3.0 MHz/i6SX1 probe; Canon Medical Systems), Vivid E9 (M5S probe; GE Healthcare), iE33 (S4 probe; PHILIPS), ACUSON SC2000 (4V1c probe; SIEMENS Healthcare), or ProSound F75 (UST-52127 probe; Fujifilm Healthcare) ultrasound machines.

In this study, echocardiography was conducted by sonographers of our institution under the supervision of certified cardiologists as a part of routine practice, according to international guidelines.[17] The results described in the final report were collected and retrospectively analyzed. In brief, we collected the RA diameter, RA area, diameter of the inferior vena cava, and estimated RA pressure data. The basal (RV diameter at end-diastole [RVDd-base]) and mid-level RV diameters at end-diastole and the end-diastolic and end-systolic RV areas (RVEDA and RVESA, respectively) were measured. The RV fractional area change (FAC) was calculated as ([RVEDA–RVESA]/RVEDA) × 100%. Tricuspid annular plane systolic excursion (TAPSE) was measured in M-mode. Tricuspid annular systolic velocity (pulsed tissue Doppler s wave: s') was measured as the peak longitudinal systolic velocity of the tricuspid annulus on the RV free-wall (FW) side. The tricuspid regurgitation pressure gradient was calculated from the peak tricuspid regurgitant jet velocity and the estimated systolic PA pressure (eSPAP) was calculated. TAPSE divided by eSPAP was also calculated.[25] The degree of tricuspid regurgitation was classified into mild, moderate, or severe, according to the relevant guidelines.[26] The LV eccentricity index (EI) was calculated using dimensions obtained in the parasternal LV short-axis view. The sonographers and cardiologists had access to general clinical data but were blinded to indices of RV function and RV–PA coupling.

Strain analysis was performed using the apical four-chamber view by a cardiologist (HS), according to international guidelines.[27] The two-dimensional (2D)-echo images were analyzed offline using vendor-independent analysis software (2D Strain Analysis software version TTA2.4; TomTec Imaging Systems), and the RA and RV strains and strain rates (SRs) were measured. For the RA, the end diastole was defined as the tricuspid valve closure, and we measured the RA strain and the peak RASR in the reservoir, conduit, and contraction phases. For the RV, we measured the RV free wall longitudinal peak strain (RVFW-LS) and three RVSRs: peak systolic SR, peak early diastolic SR, and peak atrial-diastolic SR. We also calculated the RVFW-LS divided by the eSPAP.[28] Similar to the routine echocardiography, the examiner was not blinded to the general clinical data but blinded to indices of RV function and RV-PA coupling. Another examiner (IT) performed the strain analysis for interobserver reproducibility analysis, and that examiner was blinded to clinical data and RV indices.

Calculation of indices for systolic/diastolic RV function and RV–PA coupling

In this study, RV end-systolic elastance (Ees) was deemed to reflect RV systolic function; τ, β, and Eed were deemed to reflect RV diastolic function (with τ representing relaxation, and both β and Eed representing RV stiffness). Also, Ees/Ea was considered to reflect RV–PA coupling. Each index was calculated as described below.

RVP waveform data obtained with the pressure catheter were analyzed offline. The means of five minimum RVPs, end-diastolic RVPs (RVEDPs), time constant of ventricular pressure decay (τ) values, and maximum isovolumic pressure (Piso) values were calculated. For the calculation of Piso, we applied the single-beat method,[29] in which mathematical curve fitting of RVP data during isovolumic contraction and relaxation were exerted using a dedicated software (LabChart Pro®, ADInstruments), as described in our previous study.[24] τ was calculated using the Weiss method.[30]

Ees was calculated using the following formula: $Ees = (Piso − Pes)/RVSV$ (1), where end systolic pressure (Pes) was calculated as $Pes = 1.65 × MPAP − 7.79$,[31] with MPAP measured using a pressure catheter. The RVSV was obtained using CMR imaging.[12]

Ea was calculated using the following equation: $Pes/RVSV$ (2).

From equations (1) and (2), Ees/Ea was calculated as follows: $Ees/Ea = Piso/Pes − 1$. RV diastolic stiffness (β) was calculated using the following equation[32]: $RVP = \alpha ([e^{RVV \times \beta}] − 1)$. To calculate α and β, we used the pressure and volume data sets at three points: (RVP, RV volume [RVV]) = (0, 0), (minimum RVP [RVP-min], RVESV), and (RVEDP, RVEDV). Here, RVP-min was standardized to 1 mmHg to eliminate measurement errors, and a modified RVEDP was used, as follows: $(1 + RVEDP − RVP\text{-}min)$.

Eed was calculated as the slope at end diastole in the diastolic pressure–volume relationship, using the following equation[15]: $Eed = \alpha \times \beta \times e^{RVEDV \times \beta}$.

Statistical analysis

Categorical data were expressed as absolute numbers (%) and continuous variables as medians (interquartile ranges) or mean ± SD. Differences between those with and without PH were described as the median and 95% confidence intervals. We exploratory examined the correlations between echocardiographic parameters and indices of RV function and of RV–PA coupling using Spearman's rank correlation coefficient (ρ). Considering the possible impact of tricuspid regurgitation, we calculated partial correlation coefficient between echocardiographic parameters and RV indices adjusted by three grades of tricuspid regurgitation using multiple logistic regression analysis. To calculate the sensitivity and specificity of echocardiographic parameters for detecting impaired RV function or RV–PA coupling, we used the normal range reported in previous reports and calculated the sensitivity, specificity, and accuracy of each echocardiographic index. We made this exploratory analysis only for echocardiographic parameters that exhibited good correlations with the reference RV indices. The intra- and interobserver reproducibility of four strain echocardiography indices (RVFW-LS, peak systolic SR, peak early diastolic SR, and peak atrial-diastolic SR) and RVFW-LS/sPAP was examined, using Bland–Altman analysis and intraclass coefficients (ICCs), in 12 randomly selected patients. Data provided by HS were used for intra-observer reproducibility and those by HS and IT were used for interobserver reproducibility. JMP Pro version 16 (SAS Institute Inc.) was used for statistical analysis. Statistical significance was set at $p < 0.05$.

RESULTS

Table 1 summarizes the characteristics of the 63 participants, who included 54 participants who met the criteria for PH and the nine remaining participants who did not. Table 2 shows the results of CMR imaging and RHC. CMR data were missing for four of the 63 patients, mainly because of their poor clinical condition. The calculated indices of RV function (Ees, τ, β, and Eed) and of RV–PA coupling (Ees/Ea) are summarized in Table 3 and Figure 1. Among the five indices, τ and Ees/Ea were significantly lower in the participants with PH than in those without.

The echocardiographic results of the 63 participants are summarized in Table 4. Patients with PH exhibited RV dilatation, with larger diameters and areas than those in patients without PH. The TAPSE was smaller in patients with PH. Strain analysis-derived indices of the RA and RV were generally lower in patients with PH than in those without.

The ρ of RV-related echocardiographic parameters with reference indices of RV function and of RV–PA coupling are summarized in Table 5, and those of RA or IVC-related echocardiographic parameters are summarized in Supporting Information S13: Table 2. Scatter plots of correlations between all echocardiographic parameters and indices of RV function and of RV–PA coupling are shown in the Supporting Information

TABLE 1 Characteristics of study participants.

Number of participants	63
With PH, n (%)	54 (86)
Sex, male, n (%)	25 (40)
Age, years	60 (47–70)
Body mass index (kg/m^2)	22.8 (20.1–25.9)
Concentration of brain natriuretic peptide (pg/mL)	28.6 (11.2–111.9)
Characteristics of patients with PH ($n = 54$)	
Classification of PH, Group 1/2/3/4/5, n	31/0/6/17/0
World Health Organization functional class, 1/2/3/4, n	13/15/25/1
Number of pulmonary vasodilators used, 0/1/2/3, n	23/10/10/11
Phosphodiesterase 5 inhibitor use, n (%)	27 (50)
Endothelin receptor antagonist use, n (%)	20 (37)
Prostacyclin use, oral/intravenous/ inhalative/no, n	8/7/1/38

Note: Values are expressed as frequencies or medians (ranges).
Abbreviation: PH, pulmonary hypertension.

figures. Among the echocardiographic indices examined, the highest correlation with Ees was observed for RVDd-base, and the highest correlation with τ was observed for RVESA. The correlation coefficients for Ees and τ, however, were modest with $|\rho| < 0.5$ for all echocardiographic parameters. Regarding β and Eed, the highest ρ was observed for TAPSE/ePASP and EI at end-diastole, respectively, although it remained rather low ($|\rho| < 0.4$). In contrast, Ees/Ea exhibited remarkably higher correlation coefficients with echocardiographic parameters, with RVFW-LS/eSPAP exhibiting the highest ρ at −0.72. The representative echocardiographic indices that had high correlation coefficients with the reference RV indices are shown in Figure 2. The severity of TR was classified into mild, moderate, and severe in 51, 8, and 4 patients, respectively. As shown in the Supporting Information S14: Table 3, the calculated partial correlation coefficients incorporating the severity of tricuspid regurgitation remained relatively high (≥0.49) as for the six echocardiographic parameters whose $|\rho|$ were >0.6 shown in Table 5.

Among the five RV indices, Ees/Ea most closely correlated with echocardiographic parameters. Thus, as an additional exploratory analysis, we sought to examine the diagnostic accuracy of echocardiographic parameters to detect RV–PA uncoupling. Since the lower limit of Ees/Ea is reportedly 0.7−0.8,[6,33] we used either <0.8 or <0.7 for abnormally low Ees/Ea, and subsequently calculated the area under the receiver operating characteristic curve (AUC), sensitivity, specificity, and accuracy of each echocardiographic index. As shown in Table 6, when Ees/Ea < 0.8 was used to define RV–PA uncoupling, RVFW-LS/eSPAP exhibited the highest AUC (0.88) and accuracy (0.71) with its cutoff value of −0.493. Among the other indices than strain parameters, those with AUCs > 0.80 were RVDd-base, RVESA, RVFAC, EIs, and TAPSE/eSPAP. Similarly, when Ees/Ea < 0.7 was used to define RV–PA uncoupling, RVFW-LS/eSPAP again exhibited the highest AUC at 0.87 (Supporting Information S15: Table 4).

Bland–Altman plots for intra-observer reproducibility analysis are provided in Supporting Information S11: Figure 11A. The limits of agreement were small (0.44 [−1.81 to 2.68], 0.04 [−0.2 to 0.28], −0.06 [−0.31 to 0.19], −0.02 [−0.28 to 0.22], and 0.005 [−0.046 to 0.057] for RVFW-LS, peak systolic SR, peak early diastolic SR, peak atrial-diastolic SR, and RVFW-LS/sPAP, respectively), and no systematic error was indicated. ICCs were also high, at >0.8 for the five indices (0.97, 0.92, 0.92, 0.82, and 0.99 for RVFW-LS, peak systolic SR, peak early diastolic SR, peak atrial-diastolic SR, and RVFW-LS/ sPAP, respectively). Regarding the interobserver reproducibility (Supporting Information S11: Figure 11B), limits of agreement were again small (−0.08 [−6.56 to 6.40], 0.03 [−0.35 to 0.4], −0.04 [−0.42 to 0.34], 0.01 [−0.33 to 0.34], and 0.003 [−0.17 to 0.18] for RVFW-LS, peak systolic SR, peak early diastolic SR, peak atrial-diastolic SR, and RVFW-LS/sPAP, respectively). As for peak systolic SR, the difference was small (−0.04) but the plots indicated positive proportional association. The ICCs of the five parameters were all >0.7 (0.77, 0.74, 0.81, 0.71, and 0.97 for RVFW-LS, peak systolic SR, peak early diastolic SR, peak atrial-diastolic SR, and RVFW-LS/ sPAP, respectively).

DISCUSSION

In the present study, we comprehensively compared the accuracy of echocardiographic parameters for the assessment of RV function and RV–PA coupling, using pressure catheter, CMR, and single-beat method to calculate the reference values. First, we found that Ees, the index of RV systolic function, correlated with RV diameter; and τ, the index of RV relaxation, correlated with RV end-systolic area, both with moderate correlation coefficients ($|\rho| < 0.5$). Second, β and Eed, the index of RV stiffness, did not strongly correlate with any echocardiographic parameters (all $|\rho| < 0.4$). Third, Ees/

Pulmonary Circulation Open Access

TABLE 2 Results of CMR imaging and RHC.

	All participants (n = 63)	Patients with PH (n = 54)	Patients without PH (n = 9)	Difference[a] (95% CI)
CMR imaging				
RVEDV (mL)	150.6 (123.4–197.0)[b]	164.2 (133.0–203.8)[c]	103.9 (99.5–129.9)	73.2 (45.3–101.1)
RVEDV Index (mL/m^2)	101.4 (75.4–120.6)[b]	106.4 (82.9–122.6)[c]	71.1 (67.4–77.4)	41.3 (25.6–57.0)
RVESV (mL)	92.5 (64.2–139.9)[b]	107.4 (73.7–144.8)[c]	54.6 (51.1–62.1)	68.5 (43.5–93.4)
RVESV Index (mL/m^2)	61.7 (39.1–89.5)[b]	70.3 (46.7–95.6)[c]	36.9 (34.5–39.5)	40.0 (25.2–54.7)
RVSV (mL)	53.7 (41.1–68.7)[b]	53.9 (40.6–70.8)[c]	52.3 (46.8–59.5)	4.73 (−4.77 to 14.23)
RVSV Index (mL/m^2)	35.8 (27.0–41.2)[b]	35.9 (25.2–41.5)[c]	35.4 (32.5–37.2)	1.30 (−3.46 to 6.05)
RVEF (%)	37.1 (27.4–47.4)[b]	33.9 (23.9–44.9)[c]	49.4 (42.6–53.0)	−13.4 (−19.2 to −7.7)
RHC (Swan–Ganz catheter-derived)				
PAWP (mmHg)	7 (5–9)	7 (5–9)	7 (6–9)	0 (−1 to 2)
MPAP (mmHg)	32 (23–38)	33 (27–39)	17 (14–23)	16 (12–20)
RVEDP (mmHg)	8 (6–9)	8 (6–9)	6 (5–9)	1 (−1 to 3)
MRAP (mmHg)	5 (3–6)	5 (3–6)	3 (3–5)	1 (0–3)
SV (mL)	63.0 (48.3–77.6)	62.7 (46.1–79.5)	63.0 (52.6–70.0)	1.7 (−7.7 to 11.0)
SV Index (mL/m^2)	39.4 (31.9–45.8)	38.0 (31.4–46.5)	40.7 (37.0–44.6)	−1.5 (−6.2 to 3.2)
Cardiac output (L/min)	4.14 (3.38–4.82)	4.20 (3.46–4.92)	3.89 (3.29–4.34)	0.34 (−0.33 to 1.02)
Cardiac Index (L/min/m^2)	2.60 (2.24–2.95)	2.65 (2.22–2.99)	2.55 (2.31–2.94)	0.05 (−0.30 to 0.41)
PVR (WU)	5.5 (4.0–8.0)	6.0 (4.7–8.6)	1.9 (1.8–4.0)	3.9 (2.7–5.2)
PAC (mL/mmHg)	2.03 (1.19–2.75)	1.90 (1.12–2.68)	2.54 (1.95–3.51)	−0.67 (−1.46 to 0.12)
RHC (pressure catheter-derived)				
MPAP (mmHg)	32 (24–36)	33 (27–37)	15 (14–20)	16 (12–20)
RVEDP (mmHg)	5 (3–6)	5 (3–6)	3 (2–4)	1 (0-3)
RV isovolumic pressure (mmHg)	64 (53–74)	65 (57–74)	47 (35–51)	22 (14–30)

Note: Values are expressed as medians (ranges).

Abbreviations: β, RV diastolic stiffness; τ, time constant; CI, confidence interval; CMR, cardiac magnetic resonance; Ea, arterial elastance; EDP, end diastolic pressure; EDV, end diastolic volume; Eed, end diastolic elastance; Ees, end systolic elastance; EF, ejection fraction; ESV, end systolic volume; MPAP, mean pulmonary arterial pressure; MRAP, mean right atrial pressure; PAC, pulmonary arterial compliance; PAWP, pulmonary arterial wedge pressure; PH, pulmonary hypertension; PVR, pulmonary vascular resistance; RHC, right heart catheterization; RV, right ventricle; SV, stroke volume; WU, Wood units.

[a]Differences between patients with PH and those without PH.

[b]$n = 59$.

[c]$n = 50$.

Ea, the index of RV–PA coupling, correlated well with several echocardiographic parameters, with RV FWLS/eSPAP exhibiting the best ρ at −0.72. In contrast to previous studies, through the comprehensive comparisons of many echocardiographic parameters, this study indicated the superior accuracy of RVFW-LS/eSPAP over that of other parameters, and its high sensitivity and specificity in detecting impaired RV–PA coupling.

The TAPSE, RVs′, and RVFAC are widely used echocardiographic parameters for the evaluation of RV systolic function.[17] In addition, in recent years, strain and SR indices have been reported to reflect RV systolic function.[34] However, in our study, none of these indices were significantly correlated with Ees, a reference index of RV contractility. A possible explanation for this is that TAPSE, RVs′, RVFAC, and strain indices allow the quantitative evaluation of certain aspects of RV motion, such as myocardial shortening and velocity, while Ees reflects the intrinsic contractility of the RV. Here, it should be noted that the clinical relevance of

TABLE 3 Indices of RV function and RV–PA coupling.

	All participants (n = 63)	Patients with PH (n = 54)	Patients without PH (n = 9)	Difference[a] (95% CI)
Ees (mmHg/mL)	0.40 (0.33–0.47)[b]	0.39 (0.31–0.46)[c]	0.48 (0.30–0.65)	−0.09 (−0.28 to 0.09)
τ (ms)	43.4 (40.1–46.7)	44.9 (41.5–48.3)	34.5 (24.2–44.8)	10.4 (−0.2 to 21.0)
β	0.025 (0.022–0.028)[d]	0.025 (0.022–0.029)[e]	0.024 (0.017–0.030)	0.002 (−0.005 to 0.009)
Eed (mmHg/mL)	0.12 (0.10–0.14)[d]	0.12 (0.10–0.14)[e]	0.12 (0.08–0.16)	0.01 (−0.04 to 0.05)
Ees/Ea	0.64 (0.51–0.76)	0.51 (0.42–0.60)	1.40 (0.87–1.93)	−0.89 (−1.42 to −0.36)

Note: Values are expressed as averages ± SD.

Abbreviations: CI, confidence interval; Ea, arterial elastance; Eed, end diastolic elastance; Ees, end systolic elastance; PA, pulmonary artery; RV, right ventricular.
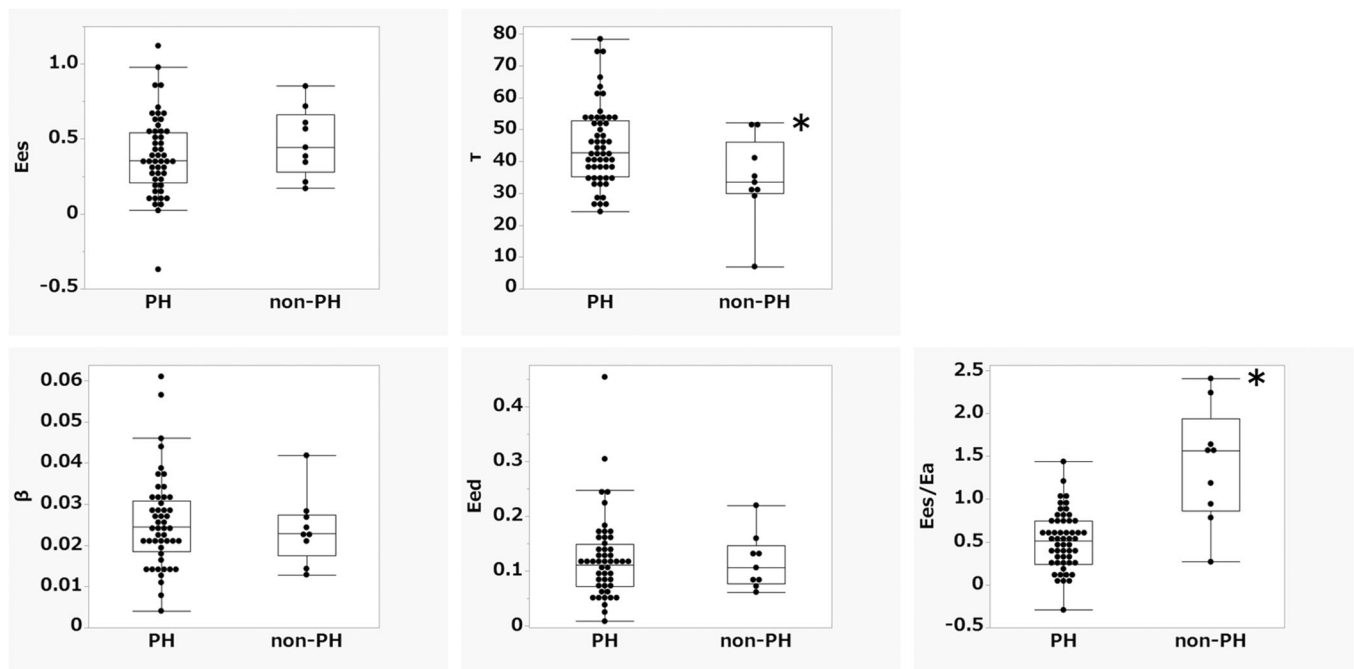
[a]Differences between patients with PH and those without PH.

[b]n = 59.

[c]n = 50.

[d]n = 58.

[e]n = 49.

FIGURE 1 Five indices of RV function and RV–PA coupling in patients with or without PH. *$p < 0.05$ versus patients with PH; differences between patients with PH and those without PH: Ees, −0.09 (−0.28 to 0.09) (mmHg/mL); τ, 10.4 (−0.2 to 1.0) (ms); β, 0.002 (−0.005 to 0.009); Eed, 0.01 (−0.04 to 0.05) (mmHg/mL); Ees/Ea, −0.89 (−1.42 to −0.36). β, RV diastolic stiffness; τ, time constant of ventricular pressure decay; Ea, atrial elastance; Eed, end diastolic elastance; Ees, end systolic elastance; PA, pulmonary artery; PH, pulmonary hypertension; RV, right ventricle.

abovementioned echocardiographic parameters has been reported in a number of studies, which is not the case for Ees. Thus, further studies are necessary to examine how echocardiography should be used for the assessment of RV systolic function in the clinical practice.

RV diastolic function can be assessed relative to relaxation and stiffness.[32] Relaxation is an active dilatory movement of the RV and can be mathematically represented as τ.[35] With echocardiography, the rate of

RVP decline during early diastole and strain indices are expected to reflect RV relaxation.[17] However, these variables were at best weakly correlated with τ. Alternatively, RV stiffness may be reflected by β and Eed, and some RA and RV indices were expected to correlate with β and Eed. Once more contrary to our expectations, none of the echocardiographic indices correlated with the two parameters, with $\rho > 0.4$. In addition, a recent study reported a significant correlation

Pulmonary Circulation

TABLE 4 Results of echocardiography.

	All participants (n = 63)	Patients with PH (n = 54)	Patients without PH (n = 9)	Difference[a] (95% CI)
2D, M-mode, and Doppler analysis				
RA and IVC indices				
RAD-long axis (mm)	48 (44–55)	49 (45–55)	46 (43–50)	5 (1–8)
RAD-short axis (mm)	37 (34–45)	38 (34–47)	36 (34–39)	5 (1–9)
RA area (cm^2)	15.8 (13.7–20.6)	16.0 (13.6–22.4)	14.9 (13.4–16.0)	3.7 (0.7–6.7)
IVC diameter (mm)	14 (11–15)	14 (11–15)	13 (10–15)	1 (−1 to 4)
RV and LV indices				
RVDd-base (mm)	42 (36–49)	42 (38–50)	35 (33–41)	8 (4–12)
RVDd-mid (mm)	32 (28–40)	34 (29–41)	27 (24–34)	6 (1–11)
RVEDA (cm^2)	21.6 (18.4–28.1)	22.5 (19.2–28.8)	17.0 (12.5–22.4)	7.5 (3.1–12.0)
RVESA (cm^2)	15.0 (12.3–21.6)	16.8 (13.1–23.1)	9.7 (7.6–14.2)	8.1 (5.0–11.2)
RVFAC (%)	27.1 (18.1–35.8)	26.4 (16.9–32.1)	36.6 (30.7–44.6)	−12.0 (−19.5 to −4.6)
TAPSE (mm)	18 (15–21)	18 (14–20)	22 (20–22)	−3 (−5 to −1)
RVs′ (cm/s)	10.5 (9.0–12.5)[b]	10.4 (8.9–12.5)[c]	13.9 (10.4–16.5)[d]	−2.7 (−7.8 to 2.3)
EId	1.09 (1.04–1.21)	1.09 (1.04–1.23)	1.12 (1.05–1.15)	0.02 (−0.04 to 0.07)
EIs	1.37 (1.08–1.72)	1.44 (1.16–1.76)	1.08 (1.07–1.21)	0.31 (0.12–0.50)
TAPSE/eSPAP (mm/mmHg)	0.408 (0.228–0.560)[e]	0.343 (0.202–0.497)[f]	0.688 (0.478–0.922)	−0.311 (−0.508 to −0.114)
RVs′/RA area index	1.03 (0.76–1.36)[b]	1.03 (0.75–1.36)[c]	1.18 (0.94–1.61)[d]	−0.17 (−0.71 to 0.37)
Strain and SR indices				
RA indices				
RAS-reservoir (%)	38.0 (28.2–49.6)[g]	35.2 (25.9–45.4)[b]	48.9 (37.1–60.4)[h]	−12.7 (−22.6 to −2.9)
RAS-conduit (%)	18.0 (12.6–23.9)[i]	16.3 (11.6–21.9)[j]	24.7 (17.9–30.5)[h]	−6.7 (−13.6 to 0.1)
RAS-contraction (%)	18.6 (13.9–22.5)[g]	18.1 (13.5–22.1)[j]	21.7 (17.3–25.9)[h]	−2.6 (−10.8 to 5.6)
Peak RASR-reservoir (/s)	1.10 (0.84–1.36)[g]	1.04 (0.83–1.36)[b]	1.19 (1.03–1.40)[h]	−0.10 (−0.30 to 0.10)
Peak RASR-conduit (/s)	−0.72 (−0.90 to −0.56)[k]	−0.70 (−0.86 to −0.50)[l]	−0.87 (−1.08 to −0.64)[h]	0.22 (−0.01 to 0.46)
Peak RASR-contraction (/s)	−0.89 (−1.27 to −0.72)[g]	−0.89 (−1.27 to −0.73)[b]	−0.89 (−1.42 to −0.66)[h]	0.03 (−0.39 to 0.45)

TABLE 4 (Continued)

	All participants (n = 63)	Patients with PH (n = 54)	Patients without PH (n = 9)	Difference[a] (95% CI)
RV indices				
RV free wall-LS (%)	−18.4 (−23.1 to −13.3)[e]	−17.5 (−21.6 to −12.6)[f]	−27.1 (−33.2 to −22.9)	10.2 (5.2–15.2)
RV free wall-LSR				
Peak systolic (/s)	−0.87 (−1.13 to −0.62)[e]	−0.82 (−1.04 to −0.61)[e]	−1.28 (−1.84 to −1.06)	0.57 (0.25–0.89)
Early diastolic (/s)	0.69 (0.37–0.87)[m]	0.67 (0.35–0.86)[l]	1.08 (0.67–1.20)	−0.32 (−0.54 to −0.09)
Late diastolic (/s)	0.66 (0.53–0.91)[e]	0.63 (0.48–0.79)[f]	1.05 (0.58–1.25)	−0.27 (−0.55 to 0.02)
RV free wall-LS/eSPAP (%/mmHg)	−0.379 (−0.682 to −0.229)[g]	−0.329 (−0.504 to −0.190)[j]	−0.972 (−1.077 to −0.741)	0.513 (0.301–0.725)

Abbreviations: 2D, two-dimensional; CI, confidence interval; EId, eccentricity index at end diastole; EIs, eccentricity index at end systole; eSPAP, estimated systolic pulmonary arterial pressure; IVC, inferior vena cava; LS, longitudinal strain; LSR, longitudinal strain rate; PH, pulmonary hypertension; RA, right atrium; RAD, RA diameter; RAS, RA strain; RASR, RA strain rate; RV, right ventricle; RVDd, RV diastolic diameter; RVEDA, RV end diastolic area; RVESA, RV end systolic area; RVFAC, RV fractional area change; s′, myocardial velocity during systole; SR, strain rate; TAPSE, tricuspid annular plane systolic excursion.

[a]Differences between patients with PH and those without PH.

[b]n = 51.

[c]n = 47.

[d]n = 4.

[e]n = 61.

[f]n = 52.

[g]n = 59.

[h]n = 8.

[i]n = 58.

[j]n = 50.

[k]n = 54.

[l]n = 46.

[m]n = 55.

Pulmonary Circulation
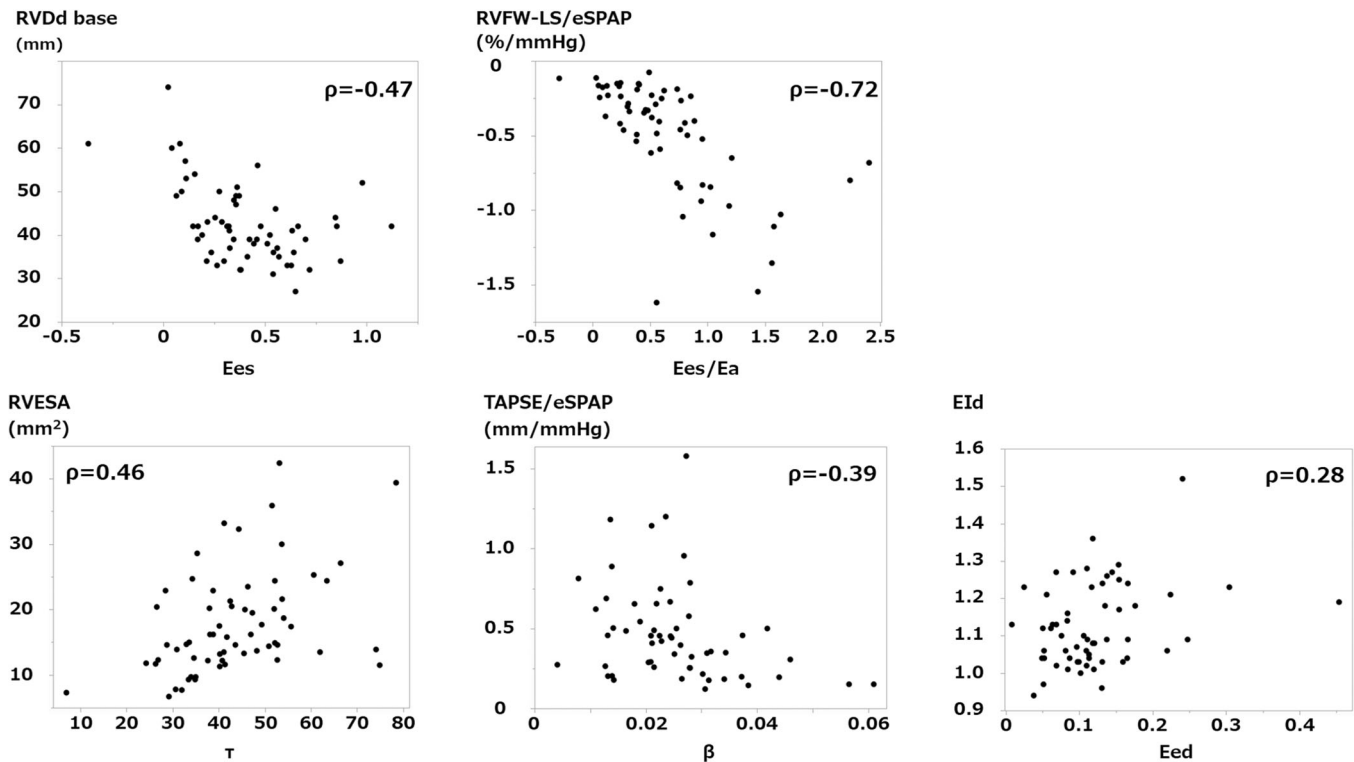
TABLE 5 Correlation coefficients (ρ) between RV-related echocardiographic parameters and indices of RV function and RV–PA coupling.

	Ees	τ	β	Eed	Ees/Ea
Echocardiographic parameters of 2D, M-mode, and Doppler analysis					
RVDd-base	−0.47 (−0.65 to −0.24)	0.40 (0.13–0.57)	0.07 (−0.22 to 0.30)	−0.05 (−0.33 to 0.19)	**−0.66** (−0.77 to −0.48)
RVDd-mid	−0.43 (−0.63 to −0.21)	0.34 (0.08–0.53)	0.07 (−0.21 to 0.30)	−0.10 (−0.38 to 0.13)	**−0.61** (−0.75 to −0.44)
RVEDA	−0.39 (−0.59 to −0.16)	0.41 (0.15–0.58)	0.03 (−0.25 to −0.26)	−0.12 (−0.39 to 0.12)	−0.54 (−0.70 to −0.34)
RVESA	−0.34 (−0.56 to −0.11)	0.46 (0.20–0.61)	0.15 (−0.14 to 0.37)	−0.08 (−0.35 to 0.16)	**−0.66** (−0.78 to −0.49)
RVFAC	0.18 (−0.08 to 0.42)	−0.36 (−0.55 to −0.11)	−0.37 (−0.57 to −0.12)	−0.11 (−0.35 to −0.16)	**0.63** (0.45–0.76)
TAPSE	0.10 (−0.17 to 0.34)	−0.13 (−0.37 to 0.12)	−0.25 (−0.48 to 0.01)	0.03 (−0.23 to 0.29)	0.45 (−0.77 to −0.48)
RVs'	0.09 (−0.21 to 0.36)	−0.26 (−0.51 to −0.01)	−0.16 (−0.43 to 0.13)	0.11 (−0.19 to 0.39)	0.28 (0.01–0.52)
EId	−0.04 (−0.30 to 0.21)	−0.03 (−0.32 to 0.18)	0.34 (0.09–0.55)	0.28 (0.02–0.50)	−0.20 (−0.43 to 0.04)
EIs	−0.08 (−0.33 to 0.18)	0.39 (0.14 to 0.57)	0.29 (0.04–0.51)	0.10 (−0.17 to 0.34)	−0.58 (−0.73 to −0.40)
TAPSE/eSPAP	0.12 (−0.63 to −0.21)	−0.31 (−0.50 to −0.03)	−0.40 (−0.60 to −0.15)	−0.17 (−0.42 to 0.09)	**0.68** (0.51–0.79)
RVs'/RA area index	0.25 (−0.03 to 0.51)	−0.32 (−0.55 to −0.05)	−0.13 (−0.40 to 0.18)	0.15 (−0.14 to 0.43)	0.48 (0.23–0.66)
Echocardiographic parameters of strain and SR analysis					
RV-free wall-LS	−0.15 (−0.40 to 0.11)	0.42 (0.15–0.59)	0.21 (−0.06 to 0.45)	−0.08 (−0.34 to 0.18)	**−0.62** (−0.75 to −0.43)
RV-free wall-LSR					
Peak systolic	−0.13 (−0.38 to 0.13)	0.44 (0.19–0.61)	0.15 (−0.13 to 0.39)	−0.11 (−0.37 to 0.15)	−0.55 (−0.71 to −0.35)
Early diastolic	0.05 (−0.24 to 0.31)	−0.36 (−0.57 to −0.09)	−0.23 (−0.47 to 0.06)	0.09 (−0.19 to 0.36)	0.50 (0.26–0.67)
Late diastolic	0.22 (−0.04 to 0.44)	−0.32 (−0.56 to −0.12)	0.03 (−0.23 to 0.30)	0.17 (−0.10 to 0.42)	0.20 (−0.06 to 0.43)
RV-free wall-LS/eSPAP	−0.15 (−0.40 to 0.12)	0.41 (−0.55 to −0.11)	0.35 (0.08–0.56)	0.11 (−0.17 to 0.36)	**−0.72** (−0.82 to −0.57)

Note: Bold numbers indicate |ρ| ≥ 0.6. Values are presented as ρ (95% confidence interval).

Abbreviations: β, RV diastolic stiffness; ρ, Spearman's rank correlation coefficient; τ, time constant; 2D, two-dimensional; Ea, atrial elastance; Eed, end diastolic elastance; Ees, end systolic elastance; EIs, eccentricity index at end systole; EId, eccentricity index at end diastole; eSPAP, estimated systolic pulmonary arterial pressure; LS, longitudinal strain; LSR, longitudinal strain rate; RV, right ventricle; RVDd, RV diastolic diameter; RVEDA, RV end diastolic area; RVESA, RV end systolic area; RVFAC, RV fractional area change; s', myocardial velocity during systole; SR, strain rate; TAPSE, tricuspid annular plane systolic excursion.

FIGURE 2 Correlations of five indices of RV function and RV-PA coupling with echocardiographic parameters with the highest correlation coefficient. β, RV diastolic stiffness; ρ, Spearman's rank correlation coefficient; τ, time constant; Ea, atrial elastance; Eed, end diastolic elastance; Ees, end systolic elastance; EId, eccentricity index at end diastole; ESA, end systolic area; PA, pulmonary artery; RV, right ventricle; RVDd, RV diastolic diameter; RVFW-LS, RV free-wall longitudinal strain; SPAP, systolic pulmonary arterial pressure; TAPSE, tricuspid annular plane systolic excursion.

of s'/[RA area index] with Eed.[20] However, in our study, there was no such good correlation between s'/[RA area index] and Eed. The difference between the two studies may be due to different methods for calculating Eed, that is, Yogaswaran et al. used a conductance catheter to measure RV volumes, whereas we used CMR data. Additionally, differences in the study participants' characteristics may have caused different results between the two studies. Thus, currently, the accuracy of echocardiographic indices for the assessment of RV diastolic function, particularly RV stiffness, is considered limited.

Echocardiographic parameters that specifically reflect RV–PA coupling are not prevalently applied in the practice; however, TAPSE/eSPAP[19,36] and RVFW-LS/eSPAP[28] are indices that show promise in this regard. Theoretically, these two measures are consistent with Ees/Ea in that both are calculated by correcting RV systolic function-related parameters (TAPSE or RVFW-LS) according to afterload (eSPAP). In the current study, we were able to show close correlations of TAPSE/eSPAP and RVFW-LS/eSPAP with Ees/Ea, consistent with recent validation studies.[19,21] In addition, application of the cut-off value of −0.493 for RVFW-LS/eSPAP yielded

high sensitivity and specificity in detecting RV–PA uncoupling, further indicating the clinical usefulness of RVFW-LS/eSPAP. Of note, however, 95% confidence intervals of ρ and AUC of RVFW-LS/eSPAP overlapped with those of other echocardiographic parameters, indicating that the differences were not statistically significant. Even so, in contrast to previous studies, our study comprehensively compared correlations of echo-cardiographic parameters with invasively obtained reference indices, showing a favorable accuracy of RVFW-LS/eSPAP. Interestingly, we revealed that other simple indices, such as RVESA, RVFAC, and TAPSE/eSPAP, correlated well with Ees/Ea. However, we were unable to explain the underlying mechanisms of such correlations between morphological and functional data and also could not deny the possible effect of unknown confounding factors. These need to be addressed in future studies.

This study has several limitations. First, the reference values that were used were not based on the gold standard method, in which pressure and conductance catheters are simultaneously used. However, our simplified method enabled us to obtain reference values from more than 50 individuals including those without PH. Second, even for use with simplified methods, the sample

TABLE 6 Receiver operating characteristic curve analysis of echocardiographic indices to detect RV–PA uncoupling.

	Ees/Ea < 0.8 defined as impaired RV–PA coupling				
	AUC (95% CI)	Cutoff value	Sensitivity	Specificity	Accuracy
Echocardiographic parameters of 2D, M-mode, and Doppler analysis					
RVDd-base	0.80 (0.65–0.90)	≥41	0.72	**0.88**	0.60
RVDd-mid	0.75 (0.59–0.86)	≥31	0.72	0.69	0.41
TAPSE	0.68 (0.50–0.82)	≤19	0.74	0.63	0.37
RVs′	0.61 (0.39–0.80)	≤12	0.75	0.55	0.30
RVEDA	0.71 (0.54–0.84)	≥16	**0.98**	0.38	0.35
RVESA	**0.81 (0.66–0.91)**	≥14	0.74	**0.81**	0.56
RVFAC	**0.83 (0.67–0.92)**	≤32	**0.85**	**0.81**	0.66
EId	0.57 (0.42–0.71)	≥1.18	0.40	**0.88**	0.28
EIs	**0.88 (0.77–0.94)**	≥1.25	0.79	**0.88**	0.66
TAPSE/eSPAP	**0.82 (0.66–0.92)**	≤0.452	0.73	**0.88**	0.61
RVs′/RA area index	0.66 (0.47–0.81)	≤0.94	0.53	**0.82**	0.34
Strain and SR parameters					
RV free wall-LS	**0.85 (0.69–0.93)**	≥−20.7	0.76	**0.88**	0.63
Peak systolic	**0.85 (0.72–0.93)**	≥−0.91	0.73	**0.94**	0.67
Early diastolic	0.80 (0.64–0.90)	≤0.73	0.75	0.80	0.55
Late diastolic	0.61 (0.43–0.77)	≤1.0	**0.89**	0.44	0.33
RV free wall-LS/eSPAP	**0.88 (0.74–0.95)**	≥−0.493	**0.84**	**0.88**	0.71

Note: Bold font indicates AUC, sensitivity, or specificity of >0.8.

Abbreviations: ρ, Spearman's rank correlation coefficient; AUC, area under the receiver operating characteristic curve; CI, confidence interval; Ees, end systolic elastance; EId, eccentricity index at end diastole; EIs, eccentricity index at end systole; eSPAP, estimated systolic pulmonary arterial pressure; LS, longitudinal strain; LSR, longitudinal strain rate; LV, left ventricle; PA, pulmonary artery; RV, right ventricle; RVD, RV diameter; RVDd, diastolic RVD; RVEDA, RV end diastolic area; RVESA, RV end systolic area; RVFAC, RV fractional area change; s′, myocardial velocity during systole; SR, strain rate; TAPSE, tricuspid annular plane systolic excursion.

size was small. Hence, we could not evaluate the impact of baseline characteristics such as age, sex, and PH subtypes on the results. In addition, although there were differences in the correlation coefficients for each echocardiographic index, the small sample size precluded us from clarifying the relevance of the differences. Third, this was a retrospective and monocentric study and, thus, was not without selection bias; therefore, care should be taken when the results are extrapolated to different populations. Fourth, for the determination of non-PH, we used the definition of mPAP < 25 mmHg without pulmonary vasodilator therapy and, thus, some patients without PH had a PVR > 3 WU, which is above that of the upper limit of PAH in the guidelines for PH published in 2015.[1] Fifth, we did not analyze all echocardiographic indices, including RV thickness and the myocardial performance index, as these require images taken specifically for those

purposes. Sixth, we used 0.8 and 0.7 as the lower limits of Ees/Ea based on previous studies; however, the relevance of using these numbers was not sufficiently validated. In this regard, we made an receiver operating characteristic (ROC) curve analysis of Ees/Ea in 30 participants (nine without PH and 21 with treatment-naïve PH) and found an optimal cut-off value of Ees/Ea at 0.77 for the discrimination of participants with and without PH. This value (0.77) was within the reported lower limit range of Eed/Ea (0.7–0.8), which supported the relevance of the ROC analysis in this study. Finally, this study was conducted only to examine the accuracy of the echocardiographic parameters, and not their clinical relevance.

In conclusion, the present exploratory analysis indicated a favorable accuracy of echocardiographic parameters for the assessment of RV–PA coupling. RVFW-LS/eSPAP exhibited the highest correlation with

the reference value, and showed high sensitivity and specificity for detecting RV–PA uncoupling. Notably, other echocardiographic parameters such as RVESA, RVFAC, EIs, and TAPSE/eSPAP also exhibited close correlations with the reference value of RV–PA uncoupling. Regarding the assessment of RV function, the accuracy of echocardiography was modest for RV systolic function and relaxation, and relatively low for RV stiffness.

AUTHOR CONTRIBUTIONS

ACKNOWLEDGMENTS

CONFLICT OF INTEREST STATEMENT

DATA AVAILABILITY STATEMENT

The data that support the findings of this study are available on request from the corresponding author.

ETHICS STATEMENT

This study was conducted in accordance with the tenets of the 1964 Declaration of Helsinki and its subsequent amendments, and was approved by the Institutional Review Board of Hokkaido University Hospital (Approval number: 016-0461). Informed consent was obtained using the opt-out method owing to the study's retrospective nature at the following site (https://www.huhp.hokudai.ac.jp/date/rinsho-johokokai/).

ORCID

Ichizo Tsujino http://orcid.org/0000-0002-0196-9572

REFERENCES

1. Galiè N, Humbert M, Vachiery JL, Gibbs S, Lang I, Torbicki A, Simonneau G, Peacock A, Vonk Noordegraaf A, Beghetti M, Ghofrani A, Gomez Sanchez MA, Hansmann G, Klepetko W, Lancellotti P, Matucci M, McDonagh T, Pierard LA, Trindade PT, Zompatori M, Hoeper M. 2015 ESC/ERS guidelines for the diagnosis and treatment of pulmonary hypertension: the Joint Task Force for the diagnosis and treatment of pulmonary hypertension of the European Society of Cardiology (ESC) and the European Respiratory Society (ERS): endorsed by Association for European Paediatric and Congenital Cardiology (AEPC), International Society for Heart and Lung Transplantation (ISHLT). Eur Respir J. 2015;46(4): 903–75.

2. Humbert M, Kovacs G, Hoeper MM, Badagliacca R, Berger R, Brida M, Carlsen J, Coats A, Escribano-Subias P, Ferrari P, Ferreira DS, Ghofrani HA, Giannakoulas G, Kiely DG, Mayer E, Meszaros G, Nagavci B, Olsson KM, Pepke-Zaba J, Quint JK, Rådegran G, Simonneau G, Sitbon O, Tonia T, Toshner M, Vachiery JL, Vonk Noordegraaf A, Delcroix M, Rosenkranz S, ESC/ERS Scientific Document G. 2022 ESC/ERS guidelines for the diagnosis and treatment of pulmonary hypertension. Eur Heart J. 2022;43(38):3618–731.

3. Humbert M, Kovacs G, Hoeper MM, Badagliacca R, Berger RMF, Brida M, Carlsen J, Coats AJS, Escribano-Subias P, Ferrari P, Ferreira DS, Ghofrani HA, Giannakoulas G, Kiely DG, Mayer E, Meszaros G, Nagavci B, Olsson KM, Pepke-Zaba J, Quint JK, Rådegran G, Simonneau G, Sitbon O, Tonia T, Toshner M, Vachiery JL, Vonk Noordegraaf A, Delcroix M, Rosenkranz S. 2022 ESC/ERS guidelines for the diagnosis and treatment of pulmonary hypertension. Eur Respir J. 2023;61(12200879):2200879.

4. Vizza CD, Lang IM, Badagliacca R, Benza RL, Rosenkranz S, White RJ, Adir Y, Andreassen AK, Balasubramanian V, Bartolome S, Blanco I, Bourge RC, Carlsen J, Camacho REC, D'Alto M, Farber HW, Frantz RP, Ford HJ, Ghio S, Gomberg-Maitland M, Humbert M, Naeije R, Orfanos SE, Oudiz RJ, Perrone SV, Shlobin OA, Simon MA, Sitbon O, Torres F, Luc Vachiery J, Wang KY, Yacoub MH, Liu Y, Golden G, Matsubara H. Aggressive afterload lowering to improve the right ventricle: a new target for medical therapy in pulmonary arterial hypertension? Am J Respir Crit Care Med. 2022;205(7):751–60.

5. Vanderpool RR, Pinsky MR, Naeije R, Deible C, Kosaraju V, Bunner C, Mathier MA, Lacomis J, Champion HC, Simon MA. RV-pulmonary arterial coupling predicts outcome in patients referred for pulmonary hypertension. Heart. 2015;101(1):37–43.

6. Richter MJ, Peters D, Ghofrani HA, Naeije R, Roller F, Sommer N, Gall H, Grimminger F, Seeger W, Tello K.

Evaluation and prognostic relevance of right ventricular-arterial coupling in pulmonary hypertension. Am J Respir Crit Care Med. 2020;201(1):116–9.

7. Hsu S, Simpson CE, Houston BA, Wand A, Sato T, Kolb TM, Mathai SC, Kass DA, Hassoun PM, Damico RL, Tedford RJ. Multi-Beat right ventricular-arterial coupling predicts clinical worsening in pulmonary arterial hypertension. J Am Heart Assoc. 2020;9(10):e016031.

8. Kass DA. Measuring right ventricular volumes. Am J Physiol Heart Circ Physiol. 1988;254(4 Pt 2):H619–21.

9. Kass DA, Maughan WL, Guo ZM, Kono A, Sunagawa K, Sagawa K. Comparative influence of load versus inotropic states on indexes of ventricular contractility: experimental and theoretical analysis based on pressure-volume relationships. Circulation. 1987;76(6):1422–36.

10. Tedford RJ, Mudd JO, Girgis RE, Mathai SC, Zaiman AL, Housten-Harris T, Boyce D, Kelemen BW, Bacher AC, Shah AA, Hummers LK, Wigley FM, Russell SD, Saggar R, Saggar R, Maughan WL, Hassoun PM, Kass DA. Right ventricular dysfunction in systemic sclerosis-associated pulmonary arterial hypertension. Circ Heart Failure. 2013;6(5): 953–63.

11. Sato T, Ambale-Venkatesh B, Zimmerman SL, Tedford RJ, Hsu S, Chamera E, Fujii T, Mullin CJ, Mercurio V, Khair R, Corona-Villalobos CP, Simpson CE, Damico RL, Kolb TM, Mathai SC, Lima JAC, Kass DA, Tsujino I, Hassoun PM. Right ventricular function as assessed by cardiac magnetic resonance imaging-derived strain parameters compared to high-fidelity micromanometer catheter measurements. Pulm Circ. 2021;11(4):1–10.

12. Sanz J, García-Alvarez A, Fernández-Friera L, Nair A, Mirelis JG, Sawit ST, Pinney S, Fuster V. Right ventriculo-arterial coupling in pulmonary hypertension: a magnetic resonance study. Heart. 2012;98(3):238–43.

13. Brimioulle S, Wauthy P, Ewalenko P, Rondelet B, Vermeulen F, Kerbaul F, Naeije R. Single-beat estimation of right ventricular end-systolic pressure-volume relationship. Am J Physiol Heart Circ Physiol. 2003;284(5):H1625–30.

14. Trip P, Kind T, van de Veerdonk MC, Marcus JT, de Man FS, Westerhof N, Vonk-Noordegraaf A. Accurate assessment of load-independent right ventricular systolic function in patients with pulmonary hypertension. J Heart Lung Transplant. 2013;32(1):50–5.

15. Trip P, Rain S, Handoko ML, van der Bruggen C, Bogaard HJ, Marcus JT, Boonstra A, Westerhof N, Vonk-Noordegraaf A, de Man FS. Clinical relevance of right ventricular diastolic stiffness in pulmonary hypertension. Eur Respir J. 2015;45(6): 1603–12.

16. Nakaya T, Ohira H, Sato T, Watanabe T, Nishimura M, Oyama-Manabe N, Kato M, Ito YM, Tsujino I. Right ventriculo-pulmonary arterial uncoupling and poor outcomes in pulmonary arterial hypertension. Pulm Circ. 2020;10(3):1–11.

17. Rudski LG, Lai WW, Afilalo J, Hua L, Handschumacher MD, Chandrasekaran K, Solomon SD, Louie EK, Schiller NB. Guidelines for the echocardiographic assessment of the right heart in adults: a report from the American Society of Echocardiography endorsed by the European Association of Echocardiography, a registered branch of the European Society of Cardiology, and the Canadian Society of Echocardiography. J Am Soc Echocardiogr. 2010;23(7):685–713.; Quiz 86–8.

18. Zaidi A, Oxborough D, Augustine DX, Bedair R, Harkness A, Rana B, Robinson S, Badano LP. Echocardiographic assessment of the tricuspid and pulmonary valves: a practical guideline from the British Society of Echocardiography. Echo Res Pract. 2020;7(4):G95–G122.

19. Tello K, Wan J, Dalmer A, Vanderpool R, Ghofrani HA, Naeije R, Roller F, Mohajerani E, Seeger W, Herberg U, Sommer N, Gall H, Richter MJ. Validation of the tricuspid annular plane systolic Excursion/Systolic pulmonary artery pressure ratio for the assessment of right ventricular-arterial coupling in severe pulmonary hypertension. Circ Cardiovasc Imaging. 2019;12(9):e009047.

20. Yogeswaran A, Rako ZA, Yildiz S, Ghofrani HA, Seeger W, Brito da Rocha B, Gall H, Kremer NC, Douschan P, Papa S, Vizza CD, Filomena D, Tedford RJ, Naeije R, Richter MJ, Badagliacca R, Tello K. Echocardiographic evaluation of right ventricular diastolic function in pulmonary hypertension. ERJ Open Res. 2023;9(5):00226–002023.

21. Richter MJ, Rako ZA, Tello K. Ratio between right ventricular strain and systolic pulmonary artery pressure as a surrogate for right ventricular to pulmonary arterial coupling: validation against the gold standard. Eur Heart J Cardiovasc Imaging. 2023;24(3):e50–2.

22. Fukuda K, Date H, Doi S, Fukumoto Y, Fukushima N, Hatano M, Ito H, Kuwana M, Matsubara H, Momomura S, Nishimura M, Ogino H, Satoh T, Shimokawa H, Yamauchi-Takihara K, Tatsumi K, Ishibashi-Ueda H, Yamada N, Yoshida S, Abe K, Ogawa A, Ogo T, Kasai T, Kataoka M, Kawakami T, Kogaki S, Nakamura M, Nakayama T, Nishizaki M, Sugimura K, Tanabe N, Tsujino I, Yao A, Akasaka T, Ando M, Kimura T, Kuriyama T, Nakanishi N, Nakanishi T, Tsutsui H. Guidelines for the treatment of pulmonary hypertension (JCS 2017/JPCPHS 2017). Circ J. 2019;83(4):842–945.

23. Rosenkranz S, Preston IR. Right heart catheterisation: best practice and pitfalls in pulmonary hypertension. Eur Respir Rev. 2015;24(138):642–52.

24. Shima H, Nakaya T, Tsujino I, Nakamura J, Sugimoto A, Sato T, Watanabe T, Ohira H, Suzuki M, Kato M, Yokota I, Konno S. Accuracy of Swan–Ganz catheterization-based assessment of right ventricular function: validation study using high-fidelity micromanometry-derived values as reference. Pulm Circ. 2022;12(2):e12078.

25. Guazzi M, Bandera F, Pelissero G, Castelvecchio S, Menicanti L, Ghio S, Temporelli PL, Arena R. Tricuspid annular plane systolic excursion and pulmonary arterial systolic pressure relationship in heart failure: an index of right ventricular contractile function and prognosis. Am J Physiol Heart Circ Physiol. 2013;305(9):H1373–81.

26. Zoghbi WA, Adams D, Bonow RO, Enriquez-Sarano M, Foster E, Grayburn PA, Hahn RT, Han Y, Hung J, Lang RM, Little SH, Shah DJ, Shernan S, Thavendiranathan P, Thomas JD, Weissman NJ. Recommendations for noninvasive evaluation of native valvular regurgitation. J Am Soc Echocardiogr. 2017;30(4):303–71.

27. Badano LP, Kolias TJ, Muraru D, Abraham TP, Aurigemma G, Edvardsen T, D'Hooge J, Donal E, Fraser AG, Marwick T,

Mertens L, Popescu BA, Sengupta PP, Lancellotti P, Thomas JD, Voigt JU, Prater D, Chono T, Mumm B, Houle H, Healthineers S, Hansen G, Abe Y, Pedri S, Delgado V, Gimelli A, Cosyns B, Gerber B, Flachskampf F, Haugaa K, Galderisi M, Cardim N, Kaufmann P, Masci PG, Marsan NA, Rosca M, Cameli M, Sade LE. Standardization of left atrial, right ventricular, and right atrial deformation imaging using two-dimensional speckle tracking echocardiography: a consensus document of the EACVI/ASE/Industry Task Force to standardize deformation imaging. Eur Heart J Cardiovasc Imaging. 2018;19(6):591–600.

28. Unlu S, Bezy S, Cvijic M, Duchenne J, Delcroix M, Voight J-U. Right ventricular strain related to pulmonary artery pressure predicts clinical outcome in patients with pulmonary arterial hypertension. Eur Heart J Cardiovasc Imaging. 2022;24(5):635–42.

29. Bellofiore A, Vanderpool R, Brewis MJ, Peacock AJ, Chesler NC. A novel single-beat approach to assess right ventricular systolic function. J Appl Physiol. 2018;124(2):283–90.

30. Weiss JL, Frederiksen JW, Weisfeldt ML. Hemodynamic determinants of the time-course of fall in canine left ventricular pressure. J Clin Invest. 1976;58(3):751–60.

31. Singh I, Oakland H, Elassal A, Heerdt PM. Defining end-systolic pressure for single-beat estimation of right ventricle-pulmonary artery coupling: simple but not really. ERJ Open Res. 2021;7(3):00219–002021.

32. Rain S, Handoko ML, Trip P, Gan CTJ, Westerhof N, Stienen GJ, Paulus WJ, Ottenheijm CAC, Marcus JT, Dorfmüller P, Guignabert C, Humbert M, MacDonald P, dos Remedios C, Postmus PE, Saripalli C, Hidalgo CG, Granzier HL, Vonk-Noordegraaf A, van der Velden J, de Man FS. Right ventricular diastolic impairment in patients with pulmonary arterial hypertension. Circulation. 2013;128(18):2016–25.

33. Tello K, Dalmer A, Axmann J, Vanderpool R, Ghofrani HA, Naeije R, Roller F, Seeger W, Sommer N, Wilhelm J, Gall H, Richter MJ. Reserve of right ventricular-arterial coupling in the setting of chronic overload. Circ Heart Failure. 2019;12(1):e005512.

34. Lee JH, Park JH. Strain analysis of the right ventricle using two-dimensional echocardiography. J Cardiovasc Imaging. 2018;26(3):111–24.

35. Murch SD, La Gerche A, Roberts TJ, Prior DL, MacIsaac AI, Burns AT. Abnormal right ventricular relaxation in pulmonary hypertension. Pulm Circ. 2015;5(2):370–5.

36. Tello K, Axmann J, Ghofrani HA, Naeije R, Narcin N, Rieth A, Seeger W, Gall H, Richter MJ. Relevance of the TAPSE/PASP ratio in pulmonary arterial hypertension. Int J Cardiol. 2018;266:229–35.

SUPPORTING INFORMATION

Additional supporting information can be found online in the Supporting Information section at the end of this article.